

TOWARD THE SIMULATION OF ATTENUATION: OSCILLATORY FLOW IN POROUS ROCK

John F. Olson

Earth Resources Laboratory
Department of Earth, Atmospheric, and Planetary Sciences
Massachusetts Institute of Technology
Cambridge, MA 02139

ABSTRACT

Fluid flow in porous rock due to an oscillatory pressure gradient is simulated. We observe distributions of density and velocity in the rock which point to viscous dissipation. We will use this method to seek a deeper understanding of the physics of attenuation.

INTRODUCTION

The attenuation of acoustic waves propagating through rock depends on the fluids present in the pores of the rock (Johnston *et al.*, 1979; Murphy *et al.*, 1986). We seek, therefore, to understand attenuation better so that we can learn more about these fluids. Attenuation takes place on the scale of pores, so it has been necessary to make assumptions about the geometry of the pores in order to develop theoretical models. Two such models are the Biot model (Biot, 1956a; Biot, 1956b) and the "squirt-flow" model (Mavko and Nur, 1979; Miksis, 1988), both of which have been fruitful. However, because the pore geometry in real rocks is more complex than any of the model geometries, it remains uncertain which model is more relevant for any particular case, and indeed whether either of them provides an adequate explanation for the observed attenuation.

In recent years, it has become possible to measure the three-dimensional geometry of the pore space in a rock at a resolution of a few microns, using X-ray microtomography (Kinney *et al.*, 1993; Spanne *et al.*, 1994; Lindquist *et al.*, 1996). It is thus possible now to simulate fluid flow in authentic rock geometry, and to compare this with results predicted from theory and measured in experiment. In this paper, we present preliminary simulations for a study of attenuation in sandstone. This simulation will use a *lattice-gas cellular automaton* to simulate the fluid, a technique which has had good

success in such problems (Auzerais *et al.*, 1996; Olson and Rothman, 1997).

SIMULATION METHOD

The lattice gas method has been described in detail many times (d’Humières and Lallemand, 1986; Frisch *et al.*, 1987; Rothman and Zaleski, 1997) so we will give only a brief outline here. In a lattice gas, the fluid is represented not as a continuum, but as a mass of identical, point particles. These particles are confined to a regular lattice in space, and they move in regular intervals of time. Particles have momentum, but while the momenta can point in different directions, they all have the same magnitude. This magnitude corresponds to the velocity needed to travel the distance from one node to a neighboring node in one time interval. Each node of the lattice may contain several particles, with momenta in different directions.

In each time step, each particle *propagates* to its neighboring node in the direction of its momentum; then all the particles at each node *collide*. The momentum of each particle may change, but the total momentum of each node remains constant. In the next time step, the particles propagate again, now in the directions of their new momenta. Because the collision conserves momentum, and if one chooses an appropriate lattice, it is possible to show that the average density and velocity of particles satisfies the Navier-Stokes equations:

$$\vec{\nabla} \cdot \vec{u} = 0 \quad \text{and} \quad \rho \frac{\partial \vec{u}}{\partial t} + \rho g(\rho) \vec{u} \cdot \vec{\nabla} \vec{u} = -\vec{\nabla} P + \eta \nabla^2 \vec{u}, \quad (1)$$

except for the density-dependent factor $g(\rho)$ before the nonlinear term. While there are ways known to guarantee that $g(\rho) = 1$, for the present problem we will deal with slow speeds at which the nonlinear term will be unimportant, and this extra factor can be neglected.

The no-slip boundary condition on solid walls can be simulated in a simple way: some nodes are labeled as wall nodes, and the collision rule on those nodes does not conserve momentum, but simply replaces the momentum of each particle with its negative. On average, this rule creates a zero-velocity surface between the wall and the fluid, though not precisely at the wall nodes. This simple rule makes it convenient to simulate flow through the complex geometry of a pore space. We use a pore space defined by tomographic data provided by Exxon Research (Auzerais *et al.*, 1996). This pore space was measured from Fontainebleau sandstone at a resolution of $7.5\mu\text{m}$. The data is gridded into cubic voxels, so we simply identify each voxel with a lattice node, although it might be wiser to identify each data voxel with a set of lattice nodes.

In the present simulations, the solid medium is perfectly rigid. We do not model elastic motions of the rock at all, but concentrate solely on fluid motion. We feel that this is an important case in its own right, since there are many circumstances under which the rock motion and the dissipation due to that motion, will be very much smaller than the motion of the fluid. We do, however, hope eventually to develop simulations of fully coupled rock and fluid motion.

Oscillatory Flow in Porous Rock

Pressure Forcing

In much previous work using lattice gases for fluid simulation, a body force was applied to the fluid by adding momentum to random nodes. For the present work, we need a new forcing scheme to simulate a pressure drop across the porous medium. The lattice gas has an equation of state analogous to the ideal gas law: the pressure of the fluid is proportional to the density, and the proportionality constant is the square of the speed of sound (Frisch *et al.*, 1987). That is, $P = c_s^2 \rho$, and the speed of sound in this case is $c_s = 1/\sqrt{2}$ lattice spacings per time step. Thus we can create a pressure gradient by adjusting the concentration of particles. It turns out that the concentration difference need be only a few percent, so the incompressible Navier-Stokes equations remain a sensible approximation.

The simulation is set up as follows: We declare a lattice of $X \times Y \times Z$ nodes, and read rock geometry data into all the nodes with $1 < x < X$: that is, we leave the extreme left and right planes empty of solid. These empty planes will be the forcing buffers, as shown in Figure 1. Because the simulation engine assumes periodic boundaries, we also wrap walls around the simulation volume, but that is only a technical detail.

On each time step, then, after colliding the particles, we adjust the pressure in the buffers by moving particles from the low-pressure side to the high-pressure side until the difference in pressures between the two buffers equals ΔP , the pressure difference we have chosen to maintain. We then continue to the next time step. As shown in Figure 2, this sets up a pressure gradient across the medium.

Oscillatory Forcing

In order to simulate an acoustic wave propagating through the medium, we generate an oscillatory pressure field in the simulation simply by changing the imposed pressure difference ΔP sinusoidally in time, that is

$$\begin{aligned}\Delta P &= P_{\text{Left}} - P_{\text{Right}} \\ &= A \sin \omega t.\end{aligned}\tag{2}$$

Because the lattice gas consists of discrete particles and corresponds to fluid dynamics only on average, we must take care to find a meaningful way to average the data. If the forcing were steady, we could wait for a steady state and then average over many time steps at that steady state; but with oscillatory forcing, there is no steady state. Instead, we use a “stroboscopic” measurement technique: we average densities and velocities not at every time step, but in four separate sets depending on the phase of the pressure forcing, as shown in Figure 3. In that way we can begin to see how the fluid in the rock responds to the oscillating pressure field.

We need to average over many time steps over many periods of the oscillating force to arrive at useful data. If we increase the number of stroboscopic samples per oscillation, we reduce the number of data acquired in each oscillation, so we need to run the simulation through more periods to get good data. On the other hand, if we lengthen

Olson

the period of the oscillation, we increase the number of data acquired in each oscillation, but it takes more time to sample the same number of periods. For the present simulation, we chose a period of 200 time steps, which corresponds to a laboratory frequency of several MHz. We ran two simulations for 10,000 time steps and then recorded data for the subsequent 20,000 time steps, then added both sets of data together so that each stroboscopic data set is an average over 10,000 time steps.

The simulation with steady forcing was similarly run for 10,000 time steps and then averaged over 20,000 time steps; since all of these time steps can be summed together, this case has less noise than the oscillatory cases.

PRELIMINARY RESULTS

Because of the practical constraints described above, we do not yet have data with which to do quantitative studies of dissipation. But we can do some qualitative examination of the data to look for evidence of dissipation, and we will see that this method has promise for future work. We will examine both the pressure field in the pore space and the velocity in the direction of the pressure gradient, contrasting the case with oscillatory forcing with the case of constant pressure gradient.

In both cases, we have rendered three-dimensional, false-color images of the quantity of interest, one such plot for each phase and a fifth for the constant gradient case. We do not plot every location, since most of the locations in the pore space have uninteresting values: average density, or zero velocity. Instead, we plot only those locations where the values are roughly one standard deviation larger or smaller than the most common, average values. These non-plotted values are indicated by an open box superimposed on the color key for each set of plots.

The Pressure Field

Color plate 1 shows the density field in the pore space, which is proportional to the pressure. The average density is 12, and density varies between 11.5 and 12.5, as indicated on the color key. First of all, consider the constant gradient case, at the bottom of the page. This image is relatively easy to interpret: we see high pressure imposed on the left buffer and low pressure on the right, with regions of less extreme pressure extending from each face into the interior. This is consistent with the pressure gradient shown in Figure 2. Most of the pore space in the middle of the volume is not shown, because the density there is about equal to the average density. Notable features are the low-pressure region at the front right bottom of the pore space and the high-pressure regions at the back left bottom and back left top.

Turning our attention now to the cases with oscillating forcing, the "full" phase is most like the constant gradient case, and indeed the pressure in the buffers appears to be the same in both cases. But more interesting are the contrasts. The most notable contrast is that, while there is substantial variation in pressure in the interior of the pore space under constant forcing, the interior is much more uniform under oscillatory

Oscillatory Flow in Porous Rock

forcing. This contrast reflects two things: first, pores might be connected only to one or another buffer and not to the network of pores which spans the simulation volume, so the pressure in these pores gradually becomes the same as the buffer pressure; but such pores would tend to average over the oscillating pressure. The region at front bottom right which was at uniform low pressure in the constant forcing case, is one such. Second, the uniformity of pressure in connected pores in the oscillatory case reflects the viscosity of the fluid. The pressure differences cannot propagate instantly into the interior of the pore space, so while a wide distribution of pressure has time to develop under steady forcing, the distribution is narrower under oscillatory forcing.

Direct evidence of this viscous lag is also visible in the images. If we contrast the “waxing” and “waning” phase images, there is a pore just inside the right face which is at lower pressure than the face in waning phase, and at higher pressure than the face in waxing phase. The region is not visible in either “new” or “full” phase, which means that its density must be average at those times. Hence, the pressure in this pore appears to follow the pressure of the adjacent face after a short lag. We now turn our attention to the velocity field.

The Velocity Field

The second plate shows the distribution of the x-component of velocity, that is, the component of velocity in the direction of the imposed pressure gradient. The velocity scale is between -0.01 and 0.01 in units of lattice spacing per time step, a range in which the lattice gas computes fluid dynamics reliably. We have shown only those locations with large positive and negative velocities, omitting the majority of locations where the velocity is near zero, as indicated on the color bar.

The layout of the different cases on this page is the same as for the pressure distribution page for ease of comparison. Let us begin, as with our consideration of the pressure distribution, with the constant gradient case on the bottom of the page. The velocity field is strikingly different from the pressure field: features which are prominent in the pressure field, are not present in the velocity field, and vice versa. In particular, the forcing buffers which are visible in the pressure field, do not appear at all in the velocity field. The reason for this is that extremes of pressure develop in enclosed pores, where little net flow can take place; whereas extremes of velocity can arise only in connected pores, where the pressure stays moderate. Since we do not show moderate pressures or small velocities, the two sets of images are largely complementary.

A particularly important feature of the constant gradient velocity field is the two lines of positive velocity passing through the middle of the medium. The flow is evidently organized into two channels which traverse the medium, with a region in the middle where they may mix. The other main feature of the constant gradient velocity field is the pore at the front bottom right, which was also a prominent low-pressure zone. This pore appears to be disconnected, and shows no evidence of containing a pressure gradient, so it is curious that there should be a continuous flow in it, as there appears to be.

Olson

Contrasting the constant gradient case with the "full" phase case, we see that the same geometric features remain prominent: the two channels through the middle of the medium, and the pore at the front bottom right. But while the velocities remain significant in the same regions, the organization of the velocity is quite different. The channels no longer convey fluid through the medium, but are broken in the middle with positive velocities at the edges and negative velocities in the interior.

Comparing the four phases with one another, we see that "full" and "new" phases are nicely complementary, as one would expect, and so too are the "waxing" and "waning" phases. Let us follow the fluid motion through a cycle of the forcing. At "full" phase, the velocity at the faces responds to the forcing with positive velocity, while the fluid in the interior is largely moving in the direction opposite to the imposed pressure gradient. Moving on to the "waning" phase, the interior velocity is now moving in the positive x direction, while the pressure gradient lapses through zero and changes sign. The fluid near the faces begins to have a negative velocity. In the "new" phase, the negative velocity propagates further into the medium, while the interior continues to have a positive velocity, opposite to the imposed pressure gradient; but by the "waxing" phase, the interior has caught up to the negative velocity while the surface starts to move positively again. So as with the pressure field, we see evidence for a phase lag between the interior of the pore space and the surface. This phase lag will result in viscous dissipation and consequently, attenuation of an acoustic signal.

CONCLUSIONS

We have performed simulations of flow through porous rock under both steady and oscillating pressure gradients. We show the distributions of pressure and velocity, and observe that these distributions vary with a lag behind the driving, with the lag increasing toward the interior of the pore space. We find that the pressure and velocity fields are complementary, in the sense that where one is extreme, the other is likely to be moderate. Finally, we observe that, while the flow is organized into channels under steady forcing and these channels are the location of most rapid motion under oscillating forcing, the flow is organized quite differently in the two cases.

While the visual representation of flow and pressure fields is interesting and affords some insight, our goal is to use such simulations to learn about the viscous mechanisms of attenuation. For this project, we will need many more simulations and more thorough analyses. To start with, the phase lag we observe in the velocity field is a consequence of the high frequency we have used, which appears to be analogous to ultrasonic frequencies in the laboratory. While this is an interesting case, we would like to investigate lower frequencies as well. Larger rock samples would also be valuable, since there would be more channels and consequently potential for more variety in the flow.

It is certainly possible to compute physical quantities from these simulations, such as the local viscous dissipation. We will examine a number of such quantities, guided by existing theory, and possibly develop new theories based on our observations.

Oscillatory Flow in Porous Rock

ACKNOWLEDGMENTS

The author gratefully acknowledges the support of the Earth Resources Laboratory Founding Members' Fellowship.

REFERENCES

- Auzerais, F.M., J. Dunsmuir, B.B. Ferréol, N. Martys, J. Olson, T.S. Ramakrishnan, and L.M. Schwartz, Transport in sandstone: A study based on three-dimensional microtomography, *Geophys. Res. Lett.*, *25*, 705–708, 1996.
- Biot, M.A., Theory of propagation of elastic waves in a fluid-saturated porous solid. I. low-frequency range, *J. Acoust. Soc. Am.*, *28* 168–178, 1956a.
- Biot, M.A., Theory of propagation of elastic waves in a fluid-saturated porous solid. II. higher frequency range, *J. Acoust. Soc. Am.*, *28* 179–191, 1956b.
- d’Humières, D. and P. Lallemand, Lattice gas automata for fluid mechanics, *Physica A*, *140*, 326–335, 1986.
- Frisch, U., D. d’Humières, B. Hasslacher, P. Lallemand, Y. Pomeau, and J.-P. Rivet, Lattice gas hydrodynamics in two and three dimensions, *Complex Systems*, *1*, 649–707, 1987.
- Johnston, D.H., M.N. Toksöz, and A. Timur, Attenuation of seismic waves in dry and saturated rocks: II. mechanisms, *Geophysics*, *44*, 691–711, 1979.
- Kinney, J.H., T.M. Breunig, T.L. Starr, D. Haupt, M.C. Nichols, S.R. Stock, M.D. Butts, and R.A. Saroyan, X-ray tomographic study of chemical vapor infiltration processing of ceramic composites, *Science*, *260*, 789–792, 1993.
- Lindquist, W.B., S.-M. Lee, D.A. Coker, K.W. Jones, and P. Spanne, Medial axis analysis of void structure in three-dimensional tomographic images of porous media, *J. Geophys. Res.*, *101*, 8297–8310, 1996.
- Mavko, G. and A. Nur, Wave attenuation in partially saturated rock, *Geophysics*, *44*, 161–178, 1979.
- Miksis, M.J., Effect of contact line movement on the dissipation of waves in partially saturated rocks, *J. Geophys. Res.*, *93*, 6624–6634, 1988.
- Olson, J.F. and D.H. Rothman, Two-fluid flow in sedimentary rock: simulation, transport and complexity, *J. Fluid Mech.*, *341*, 343–370, 1997.
- Rothman, D.H. and S. Zaleski, *Lattice-Gas Automata: Simple Models of Complex Hydrodynamics*, Cambridge University Press, Cambridge, 1997.
- Spanne, P., J.F. Thovert, C.J. Jacquin, W.B. Lindquist, K.W. Jones, and P.M. Adler, Synchrotron computed microtomography of porous media: topology and transports, *Physical Review Letters*, *73*, 2001–2004, 1994.
- Murphy, W.F., III, K.W. Winkler, and R.L. Kleinberg, Acoustic relaxation in sedimentary rocks: Dependence on grain contacts and fluid saturation, *Geophysics*, *51*, 757–766, 86.

Oscillatory Flow in Porous Rock

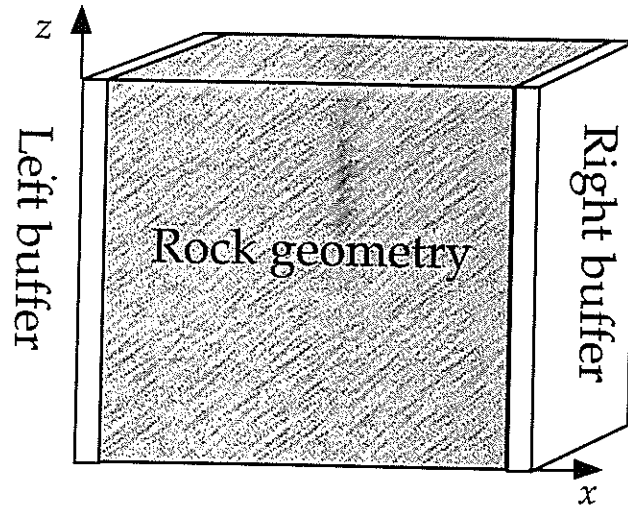


Figure 1: Simulation setup. The extreme left and right planes are empty of solid to serve as the pressure forcing buffers, and rock data fills the rest of the simulation. In fact, the simulation engine assumes a periodic geometry, so there are some additional walls omitted from this description.

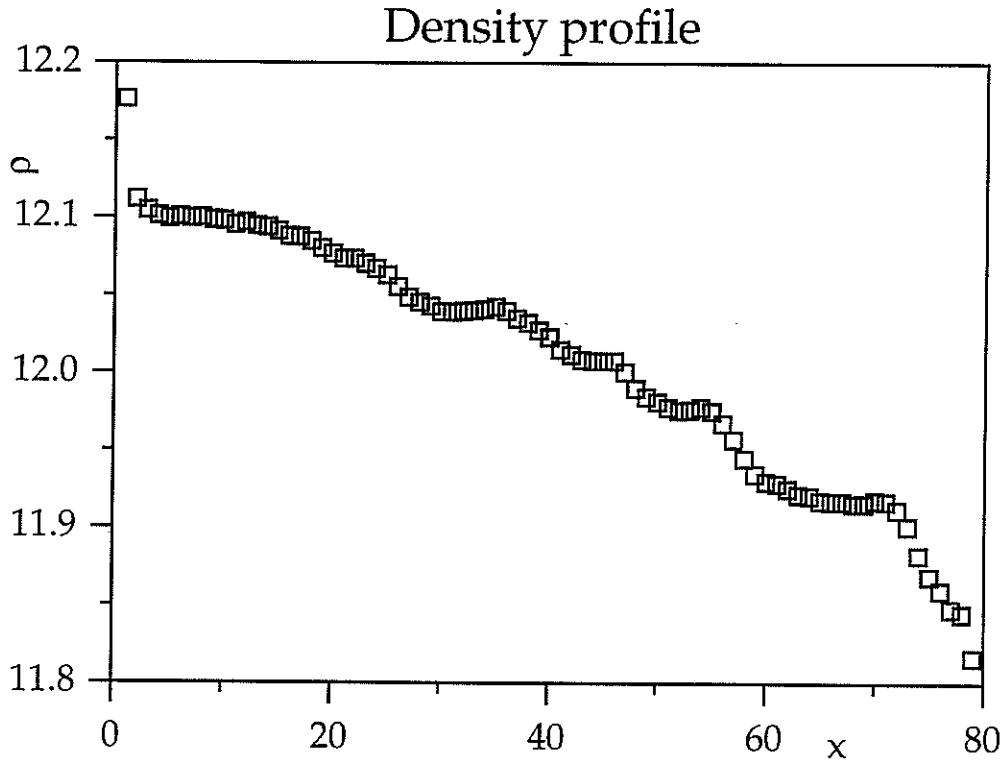


Figure 2: Pressure profile. Moving particles from the right buffer to the left buffer generates a pressure gradient across the medium, as shown above. The leftmost and rightmost data are the densities of particles in these buffers. These data were averaged over 20,000 time steps after allowing the system to come to steady state for 10,000 time steps. The gradient is not uniform because the medium is not uniform: locally steeper gradients correspond to locally constricted flow. The pressure gradient, in turn, generates a fluid flux as expected from the Darcy law. In this case, the flux corresponds to a permeability of $\approx 0.81(\mu\text{m})^2$, which is in reasonable agreement with the experimental value of $1.1(\mu\text{m})^2$.

Oscillatory Flow in Porous Rock

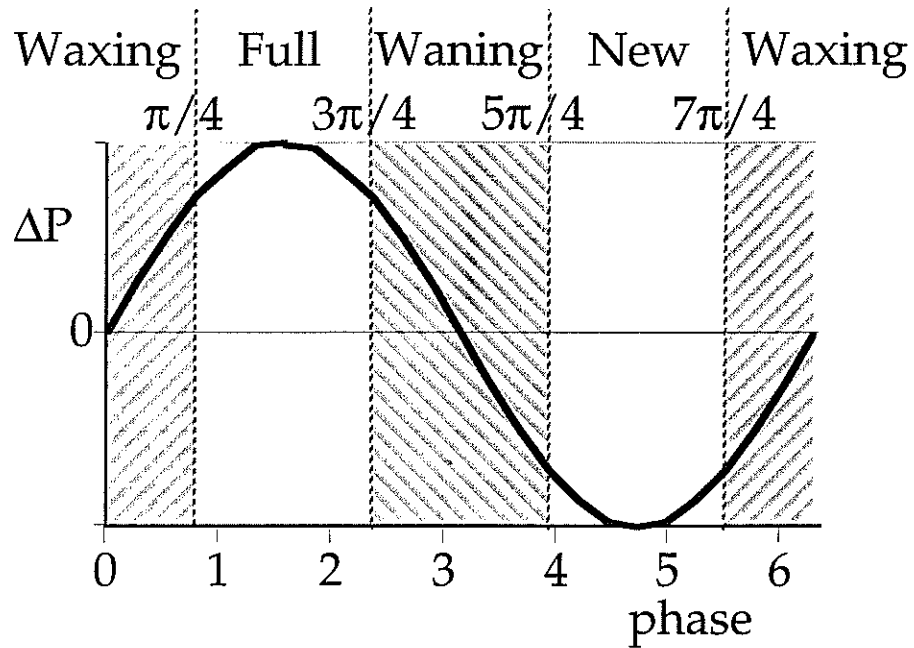
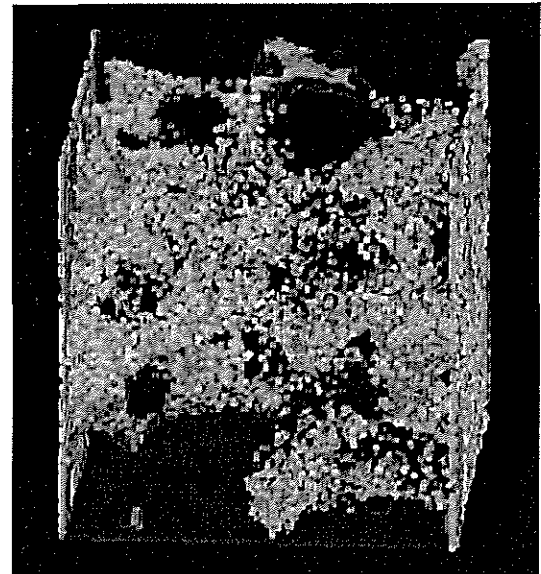
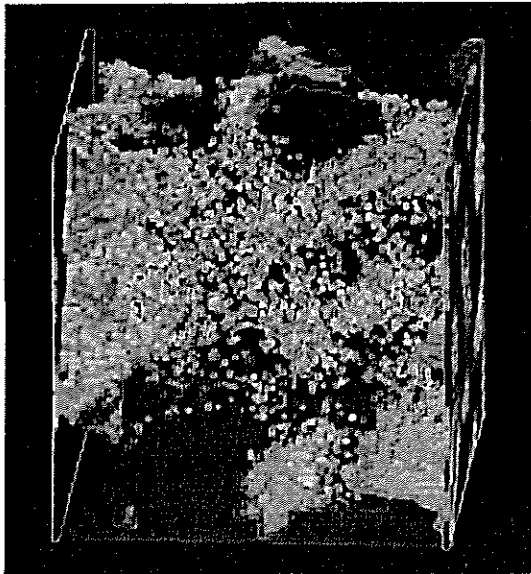


Figure 3: Stroboscopic measurement. As the pressure difference varies sinusoidally with time, we sum velocity and density information in four sets corresponding to the phase (ωt from equation 2, wrapped with a period of 2π) of the oscillation. We name these categories after the phases of the moon: Full, for when the left side has a higher pressure than the right; Waning, when the pressure on the left is decreasing and that on the right, increasing; New, the opposite of Full, and Waxing, the opposite of Waning.

New

Plate 1: Density fields

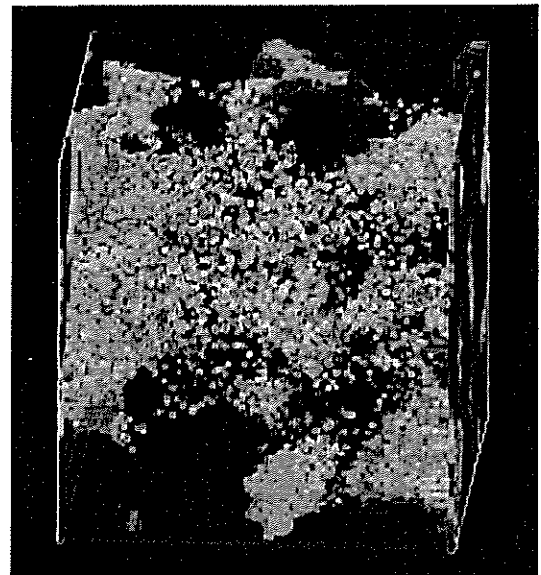
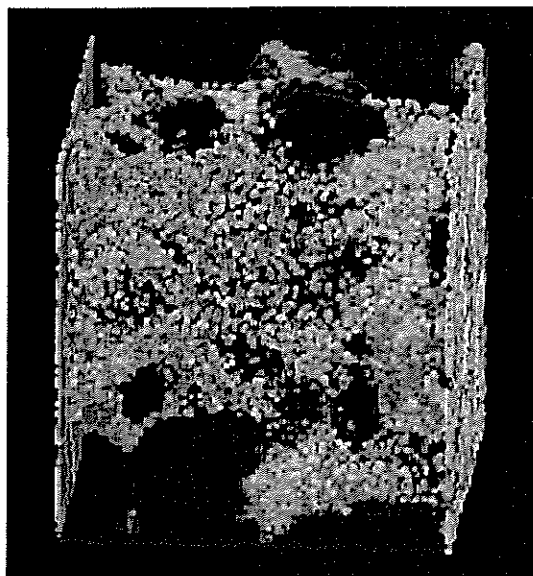
Waxing



11.5

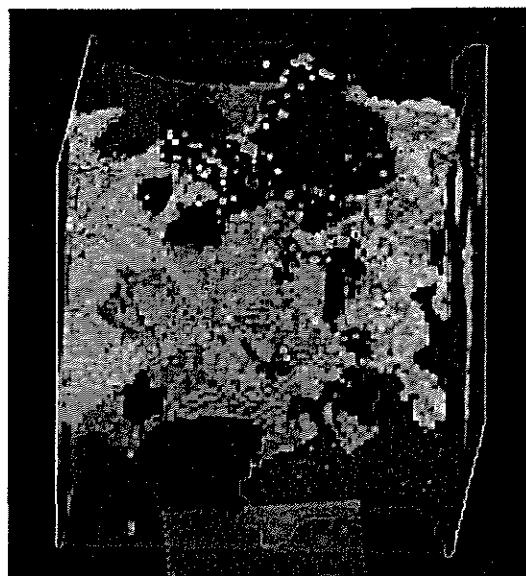
12

12.5



Waning

Full

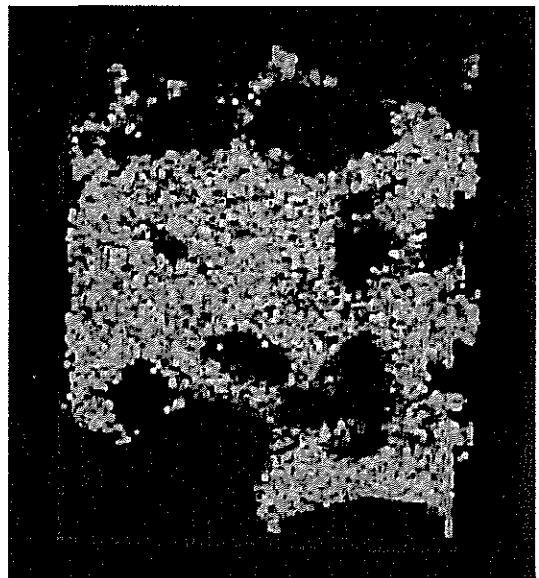
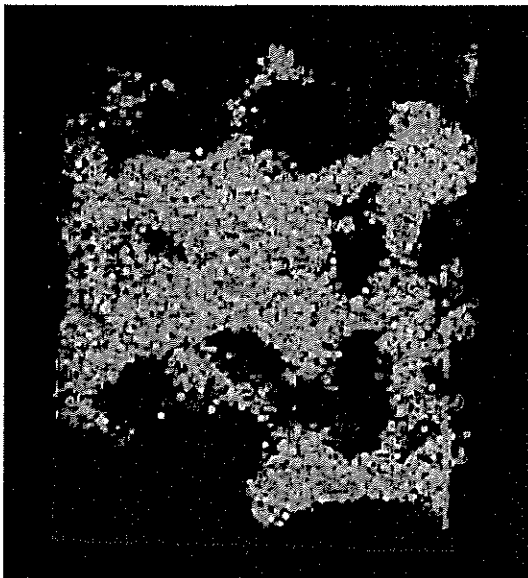
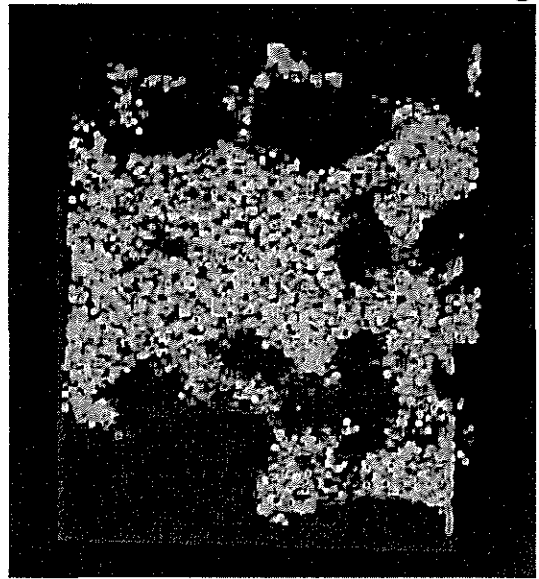
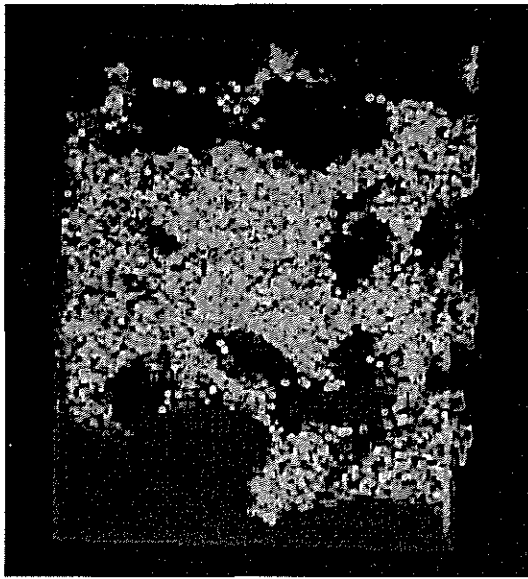


Constant
gradient

New

Plate 2: Velocity Fields

Waxing



Waning

Full



Constant
gradient

(

(

(

(

(

(

(

(

(

(

(